# Duration and Ice Thickness of a Late Holocene Outlet Glacier Advance near Narsarsuaq, South Greenland

Peter J.K. Puleo[1] and Yarrow Axford[1]

[1]Department of Earth and Planetary Sciences, Northwestern University, Evanston, 60201, USA

5  *Correspondence to*: Peter J.K. Puleo (peterpuleo2024@u.northwestern.edu)

**Abstract.** Greenland Ice Sheet (GrIS) outlet glaciers are currently losing mass leading to sea level rise. Reconstructions of past outlet glaciers through the Holocene help us better understand how they respond to climate change. Kiattuut Sermiat, a south Greenland outlet glacier near Narsarsuaq, is known to have experienced an anomalously small Little Ice Age advance compared with a larger Holocene advance that culminated at ~1600 cal yr BP. We report sedimentary records from two lakes
10  at slightly different elevations in an upland valley adjacent to Kiattuut Sermiat, which reveal when the outlet glacier was significantly larger than its Little Ice Age size and constrain the associated outlet glacier surface elevation. We use bulk sediment geochemistry, magnetic susceptibility, color, texture, and the presence of aquatic plant macrofossils to distinguish between till, glaciolacustrine sediments, and organic lake sediments. Our ^{14}C results above basal till recording regional deglaciation skew slightly old due to a hard water effect but are generally consistent with regional deglaciation occurring
15  ~11,000 cal yr BP. Neoglacial advance of Kiattuut Sermiat is recorded by deposition of glaciolacustrine sediments in the lower-elevation lake, which was subsumed by an ice-dammed lake that formed along the glacier's margin just after ~3900 cal yr BP. This timing is consistent with several other glacial records in Greenland showing Neoglacial cooling driving advance between ~4500-3000 cal yr BP. Given that glaciolacustrine sediments were deposited only in the lower-elevation lake, combined with glacial geomorphological evidence in the valley containing these lakes, we estimate the former ice margin's
20  elevation to have been ~670 m, compared with ~420 m today. The ice-dammed lake persisted until glacier retreat at ~1600 cal yr BP. That retreat timing contrasts with overall evidence for cooling and glacier advance in the region at that time, so we infer that retreat may have resulted from reduced precipitation amounts and/or local glaciological complexity. High sensitivity to precipitation changes could also explain the limited Little Ice Age advance of Kiattuut Sermiat compared to other Greenland glaciers.

## 1 Introduction

The Greenland Ice Sheet (GrIS) today is losing mass and is one of the largest contributors to global sea level rise in response to anthropogenic warming (Dowdeswell, 2006; Goelzer et al., 2020; Greve and Chambers, 2022). The amount of sea level rise contributed by the GrIS is highly dependent on future emission scenarios (Goelzer et al., 2020; Greve and Chambers, 2022).
30  Much of this mass is lost through outlet glaciers, making understanding how and why the dynamics of outlet glaciers have changed over time vital for improving estimates of future GrIS contributions to sea level rise (Goelzer et al., 2020).

The ice sheet's history during the warming and cooling phases of the Holocene provides insights into how outlet glaciers and overall ice sheet mass balance respond to climate change. Here, we focus on south Greenland, where past work has constrained aspects of the Holocene ice sheet and climate history. Increases in Northern Hemisphere summer insolation (Berger and Loutre, 1999) and greenhouse gas (Monnin et al., 2001) drove abrupt overall warming in Greenland following the Last Glacial Maximum (Buizert et al., 2018). South Greenland is also particularly sensitive to changing Atlantic Meridional Overturning Circulation conditions, like those that occurred in the Younger Dryas (~12,900-11,700 cal yr BP) and drove abrupt temperature shifts (Puleo et al., 2022). Abrupt deglacial warming led to rapid regional deglaciation around south Greenland, which occurred at ~12,300 cal yr BP near Qaqortoq (Levy et al., 2020) and ~11,100-10,500 cal yr BP near Narsarsuaq (Larsen et al., 2011; Carlson et al., 2014; Nelson et al., 2014). In the early to middle Holocene, elevated Northern Hemisphere summer insolation (Berger and Loutre, 1999) drove further warming during the Holocene Thermal Maximum (~9000-5000 cal yr BP; Axford et al. 2021). In south Greenland, the southernmost GrIS ice margin was behind its present extent for some time between ~7000 to 3000 cal yr BP in response to warmth that probably peaked in this region between ~7300 and 5500 cal yr BP (Kaplan et al., 2002; Larsen et al., 2011; Larsen et al., 2015; Larocca et al. 2020a). Subsequent Neoglacial cooling in the middle and especially late Holocene drove glacier growth around much of Greenland, including in the south (Larocca and Axford, 2022). Many glaciers reached their maximum late Holocene positions during the Little Ice Age (Larocca and Axford, 2022), but exceptions hint at complex patterns of late Holocene glacier change.

One notable exception is the Narsarsuaq advance. The Narsarsuaq advance of Kiattuut Sermiat (Kiagtût Sermiat; Bjørk et al., 2015), a southernmost GrIS outlet glacier, had a culmination timing of outermost moraines at ~1500 cal yr BP based on [10]Be and lake sediment dating (Weidick, 1963; Bennike and Sparrenbom, 2007; Winsor et al., 2014; Nelson et al., 2014). Retreat of Kiattuut Sermiat at ~1500 cal yr BP is not consistent with nearby temperature reconstructions that demonstrate cooling at this time (Wooller et al., 2004; Fréchette and de Vernal, 2009; Lasher et al., 2019). The onset timing of this advance is unconstrained and its magnitude greatly exceeded the extent of the Kiattuut Sermiat Little Ice Age advance (Winsor et al., 2014).

To determine the duration and timing of the Narsarsuaq advance, we collected sediment cores from two lakes situated within an upland valley that is tributary to the valley of Kiattuut Sermiat. This valley was partly ice-dammed by the expanded outlet glacier during the Narsarsuaq advance. Sediment records from the two threshold lakes, which sit at slightly different elevations, also allow us to precisely constrain the elevation of the outlet glacier surface (ice dam) during the period of maximum advance.

## 2 Study Area

Kiattuut Sermiat, an outlet glacier of the GrIS, is located ~10 km northeast of Narsarsuaq and is adjacent to the Mellemlandet plateau (Fig. 1B). Kiattuut Sermiat flows to the southwest and feeds the Narsarsuaq river that runs into the Tunugdliarfik fjord. Informally named lakes LMEL (Lower Mellemlandet; 61.2423°N, 45.2217°W) and UMEL (Upper Mellemlandet; 61.2373°N, 45.2282°W) are located in an east-west trending valley on Mellemlandet, an ice-free, high-elevation, northeast-southwest trending bedrock ridge that divides Kiattuut Sermiat from the adjacent outlet glacier Qooqqup Sermia (Qôrqup Sermia; Bjørk

et al., 2015; Figs. 1B, C). Satellite images and digital elevation models (DEMs) show landscape features west of the lakes, including paleoshorelines, lateral moraines, and probably subaqueous moraines, that record a time when Kiattuut Sermiat advanced into the east-west valley that contains the lakes (Figs. 1D and E). The corresponding paleoglacier's advanced position would have dammed the valley, and thus the lake system's outlet stream, and created a proglacial lake. Depending upon its

70    depth and extent, this proglacial lake could have subsumed LMEL and possibly UMEL.
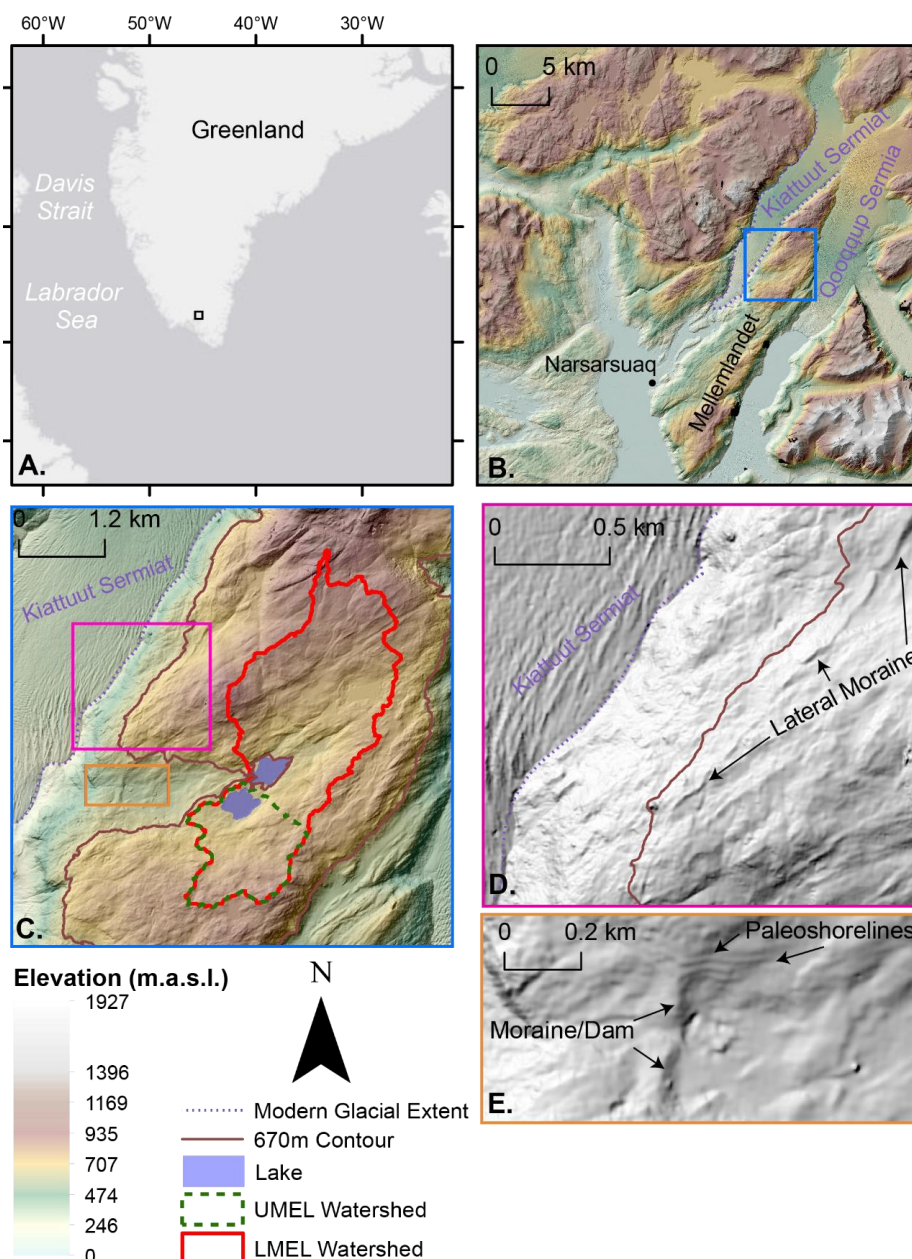
**Figure 1** (A) Map of south Greenland (ESRI). Black square shows the extent of panel B. (B) Shaded relief digital elevation model (DEM) of the region around Narsarsuaq. Blue square shows the extent of panel C. (C) DEM with LMEL and UMEL and their watersheds (in solid red and dashed green outlines, respectively). The brown line indicates the 670 m contour. Pink square shows the extent of panel D. Orange rectangle shows the extent of panel E. (D) DEM showing a lateral moraine of Kiattuut Sermiat, and 670 m contour in brown. (E) DEM showing an associated moraine and paleoshoreline features.

LMEL is 0.12 km$^2$ and has an elevation of ~670 meters above sea level (m a.s.l.). Its maximum depth is ~28 m and its watershed area is 7.0 km$^2$ (Fig. 1C). UMEL is 0.13 km$^2$ and has an elevation of ~675 m a.s.l. Its maximum depth is ~26 m and its watershed area is 1.9 km$^2$ (Fig. 1C). Both lakes have no glaciers in their watershed at present and are ~2.5 km east of (and ~250 m above the modern-day elevation of) Kiattuut Sermiat. The vegetation cover was estimated at ~70% in July 2019 and includes *Chamaenerion latifolium*, *Empetrum nigrum*, and *Betula nana*. The bedrock of the Mellemlandet ridge is largely granite and granodiorite (~1800 ma, Julianehåb igneous complex; Steenfelt et al., 2016) with some metasedimentary gneiss that may contribute ancient carbon to LMEL and UMEL.

The closest modern climate station is located in Narsarsuaq (~10 km SW of LMEL and UMEL). Mean annual air temperature in Narsarsuaq from 1981-2010 was 1.1°C (Cappelan, 2019). Mean monthly temperatures range from -7.3°C (February) to 10.8°C (July). The mean annual precipitation amount from 1981-2010 was 650.7 mm with the mean monthly precipitation amounts slightly weighted to the summer and fall. Mean temperatures at LMEL and UMEL are likely lower due to the higher elevation of the sites compared to the Narsarsuaq climate station (30 m a.s.l.).

## 3 Methods

### 3.1 Sediment Core Collecting and Sediment Characterization

In July 2019, we collected several sediment cores from LMEL and UMEL (Table 1). From LMEL, we focus on 19-LMEL-N2, 19-LMEL-U11, and 19-LMEL-U5 (recovered from 12.3, 8.0, 18.9 m water depth, respectively). These cores were selected due to their relatively long length and representation of varied water depths and locations within the lake. From UMEL, two cores were collected (19-UMEL-U2 at 12 m water depth and 19-UMEL-U1 at 24.5 m water depth). 19-LMEL-N2 was collected with a Nesje percussion piston coring device (Nesje, 1992) while the other cores were collected with an Aquatic Research Instruments "Universal" open-valve coring device designed to capture an intact sediment-water interface.

The sediment cores were split using a GeoTek core splitter and stored at 4°C. Magnetic susceptibility (MS), visible color reflectance, and elemental abundance of freshly split cores were measured every 2 mm using a Geotek MSCL-S equipped with a Bartington MS2E point sensor, a Konica Minolta CM-700d spectrophotometer, and an Olympus DELTA Professional X-Ray Fluorescence (XRF) spectrometer. Cores were topped with 4 µm Ultralene film prior to scanning. XRF measurements had a 30 second dwell time.

**Table 1** Core sampling location information. For the Core Name column: U=Universal (check valve) core and N=Nesje (piston) core.

| Lake | Core Name | Latitude (°N) | Longitude (°W) | Water Depth (m) |
|------|-----------|---------------|----------------|-----------------|
| UMEL | U1 | 61.23745 | 45.22714 | 24.5 |
| UMEL | U2 | 61.23750 | 45.22868 | 12 |
| LMEL | U5 | 61.24208 | 45.21881 | 18.9 |
| LMEL | U11 | 61.24088 | 45.22044 | 8.0 |
| LMEL | N2 | 61.24239 | 45.22174 | 12.3 |

110   Many sedimentological properties have been used to infer glacial changes based on lake sediments. Glaciers typically drive increased delivery of fine grained, minerogenic material to lakes via bedrock erosion and glacial meltwater transport. Thus, when glaciers are present in a watershed, lake waters are often turbid and aquatic primary production is low. The resulting lacustrine sediments have a relatively small amount of organic material and consist largely of minerogenic silt/clay (occasionally with some larger, unsorted grains), with these properties often clearly reflected in sediment color (Karlen and

115   Matthews, 1992; Balascio et al., 2015; Adamson et al., 2022; Larocca and Axford, 2022). Additionally, glacier-influenced lacustrine sediments are characterized by relatively large concentrations of elements found in local bedrock (e.g., Ti) and often high MS values from abundance of iron-bearing mineral grains and low abundance of biogenic materials (Karlen and Matthews, 1992; Larsen et al., 2011; Larocca et al., 2020a). Following the precedent of numerous studies in southwest/south Greenland (e.g., Larsen et al., 2011, 2015; Schweinsberg et al., 2017, 2018; Larocca et al., 2020a, 2020b), we infer glacier

120   influence on our study lakes from Ti abundance, MS, and qualitative assessments of grain size and organic content (the latter based on sediment color).

### 3.2 Sediment Core Chronology

Terrestrial plant remains, aquatic moss remains, and bulk sediments were sampled from 19-LMEL-N2 (n=7), 19-LMEL-U11

125   (n=12), 19-LMEL-U5 (n=2), and 19-UMEL-U2 (n=5) and submitted to the Woods Hole Oceanographic Institution National Ocean Sciences Accelerator Mass Spectrometry (WHOI NOSAMS) for Accelerator Mass Spectrometry ^{14}C analysis (Table 2). Most radiocarbon samples were collected just above or below clear sedimentological transitions, and we sampled terrestrial plant remains where possible to avoid potential hard water/reservoir effects. Bulk sediments were sampled as a last resort where no adequate plant macrofossils were preserved. Bulk sediment ^{14}C samples were paired with plant macrofossils at

130    several depths to evaluate the efficacy of $^{14}$C in bulk sediments. Radiocarbon ages were calibrated using Calib version 8.2

(Stuiver et al., 2022) and the IntCal20 calibration curve (Reimer et al., 2020).

**Table 2** Radiocarbon samples from LMEL and UMEL sediment cores with $^{14}$C and calibrated ages.

| Core | Sample ID | Depth in Sediment (cm) | Material | Fraction Modern | $^{14}$C Age ($^{14}$C yr BP) | $^{14}$C Age Error (2σ) | Median Cal. Age (cal yr BP) | Min. Cal. Age (cal yr BP, 2σ) | Max. Cal Age (cal yr BP, 2σ) |
|---|---|---|---|---|---|---|---|---|---|
| 19 LMEL N2 | 176106 | 7.5 | Aquatic Moss | 0.7952 | 1840 | 20 | 1740 | 1710 | 1820 |
| 19 LMEL N2 | 176107 | 8.5 | Aquatic Moss | 0.7944 | 1850 | 20 | 1760 | 1710 | 1820 |
| 19 LMEL N2 | 176110 | 210.5 | Sediment | 0.5705 | 4510 | 25 | 5150 | 5050 | 5300 |
| 19 LMEL N2 | 176111 | 217.5 | Sediment | 0.3029 | 9590 | 60 | 10,940 | 10,730 | 11,170 |
| 19 LMEL N2 | 176108 | 217.5 | Aquatic Moss | 0.2912 | 9910 | 45 | 11,310 | 11,220 | 11,600 |
| 19 LMEL N2 | 176112 | 220 | Sediment | 0.2838 | 10,100 | 50 | 11,670 | 11,400 | 11,880 |
| 19 LMEL N2 | 176109 | 220 | Aquatic Moss | 0.2767 | 10,300 | 45 | 12,070 | 11,840 | 12,460 |
| 19 LMEL U11 | 176116 | 10.5 | Aquatic Moss | 0.7795 | 2000 | 20 | 1940 | 1880 | 1990 |
| 19 LMEL U11 | 176115 | 20.5 | Aquatic Moss | 0.7298 | 2530 | 20 | 2620 | 2500 | 2740 |
| 19 LMEL U11 | 176767 | 29.25 | Terrestrial Plant | 0.8392 | 1410 | 25 | 1320 | 1290 | 1350 |
| 19 LMEL U11 | 176114 | 31.5 | Terrestrial Plant / Aquatic Moss | 0.8092 | 1700 | 15 | 1580 | 1540 | 1670 |
| 19 LMEL U11 | 176113 | 32.5 | Aquatic Moss | 0.7618 | 2190 | 25 | 2240 | 2120 | 2310 |
| 19 LMEL U11 | 176117 | 32.5 | Sediment | 0.7293 | 2540 | 20 | 2630 | 2520 | 2740 |
| 19 LMEL U11 | 176121 | 132.5 | Sediment | 0.6046 | 4040 | 25 | 4480 | 4420 | 4570 |
| 19 LMEL U11 | 176122 | 133.5 | Sediment | 0.5974 | 4140 | 20 | 4690 | 4580 | 4820 |
| 19 LMEL U11 | 176118 | 133.5 | Terrestrial Plant | 0.6410 | 3570 | 35 | 3870 | 3720 | 3980 |
| 19 LMEL U11 | 176119 | 140 | Terrestrial Plant | 0.4688 | 6090 | 35 | 6950 | 6800 | 7160 |
| 19 LMEL U11 | 176123 | 147 | Sediment | 0.4217 | 6940 | 35 | 7760 | 7680 | 7910 |
| 19 LMEL U11 | 176120 | 147 | Terrestrial Plant | 0.4874 | 5770 | 30 | 6570 | 6490 | 6660 |

| 19 LMEL U5 | 176130 | 22.5 | Sediment | 0.7787 | 2010 | 20 | 1950 | 1890 | 2000 |
|---|---|---|---|---|---|---|---|---|---|
| 19 LMEL U5 | 176129 | 23.5 | Sediment | 0.7590 | 2220 | 20 | 2230 | 2150 | 2320 |
| 19 UMEL U2 | 176128 | 18.5 | Aquatic Moss | 0.7694 | 2110 | 20 | 2070 | 2000 | 2140 |
| 19 UMEL U2 | 176127 | 36 | Terrestrial Plant | 0.7003 | 2860 | 25 | 2980 | 2880 | 3070 |
| 19 UMEL U2 | 176126 | 58 | Terrestrial Plant | 0.4079 | 7200 | 40 | 8000 | 7940 | 8170 |
| 19 UMEL U2 | 176125 | 73.5 | Aquatic Moss | 0.2939 | 9840 | 50 | 11,250 | 11,180 | 11,390 |
| 19 UMEL U2 | 176124 | 78 | Aquatic Moss | 0.2813 | 10,200 | 50 | 11,870 | 11,640 | 12,050 |

135

### 3.3 Watershed Development and Elevation History

We modeled watershed areas for LMEL and UMEL using the ESRI ARCMap Hydrology toolset and the 2 m resolution ArcticDEM (Porter et al., 2018). Modern topography, lake elevations, and watershed boundaries were used to estimate the past elevation of the Kiattuut Sermiat ice dam during periods when lake sediments reveal LMEL was subsumed by a proglacial

140 lake.

## 4 Results

### 4.1 Sediment Properties

19-LMEL-N2 is 261.5 cm long and its sediments comprise two primary units (and three subunits of Unit 1) based on changes

145 in color, grain size, presence of organic matter, MS, and sediment chemistry (Fig. 2). Unit 2 (261.5-224 cm), the lowermost unit, is a gray, poorly sorted diamicton with pebbles and granules in a matrix of silt/clay and has no visible organic materials. Much of the unit could not be scanned due to unevenness of the split core surface around its large grains; however, the uppermost part of the unit was scannable and has relatively high MS and Ti values. This lowermost unit does not have well preserved internal stratigraphy. The overlying Unit 1 comprises horizontally bedded and relatively well-sorted sediments. Unit

150 1c (224-210 cm) consists of horizontally bedded, medium brown, fine sediments with some aquatic moss remains, and low values of MS and Ti. Unit 1b (210-10 cm) is laminated to coarsely bedded, light to dark gray silt/clay without visible organics or macrofossils. It has relatively high values of MS throughout with some variability in Ti. The uppermost Unit, 1a (10-0 cm), is brown with some black laminations and contains a large amount of aquatic moss remains. The Unit 1a sediments are characterized by low MS and Ti concentrations.
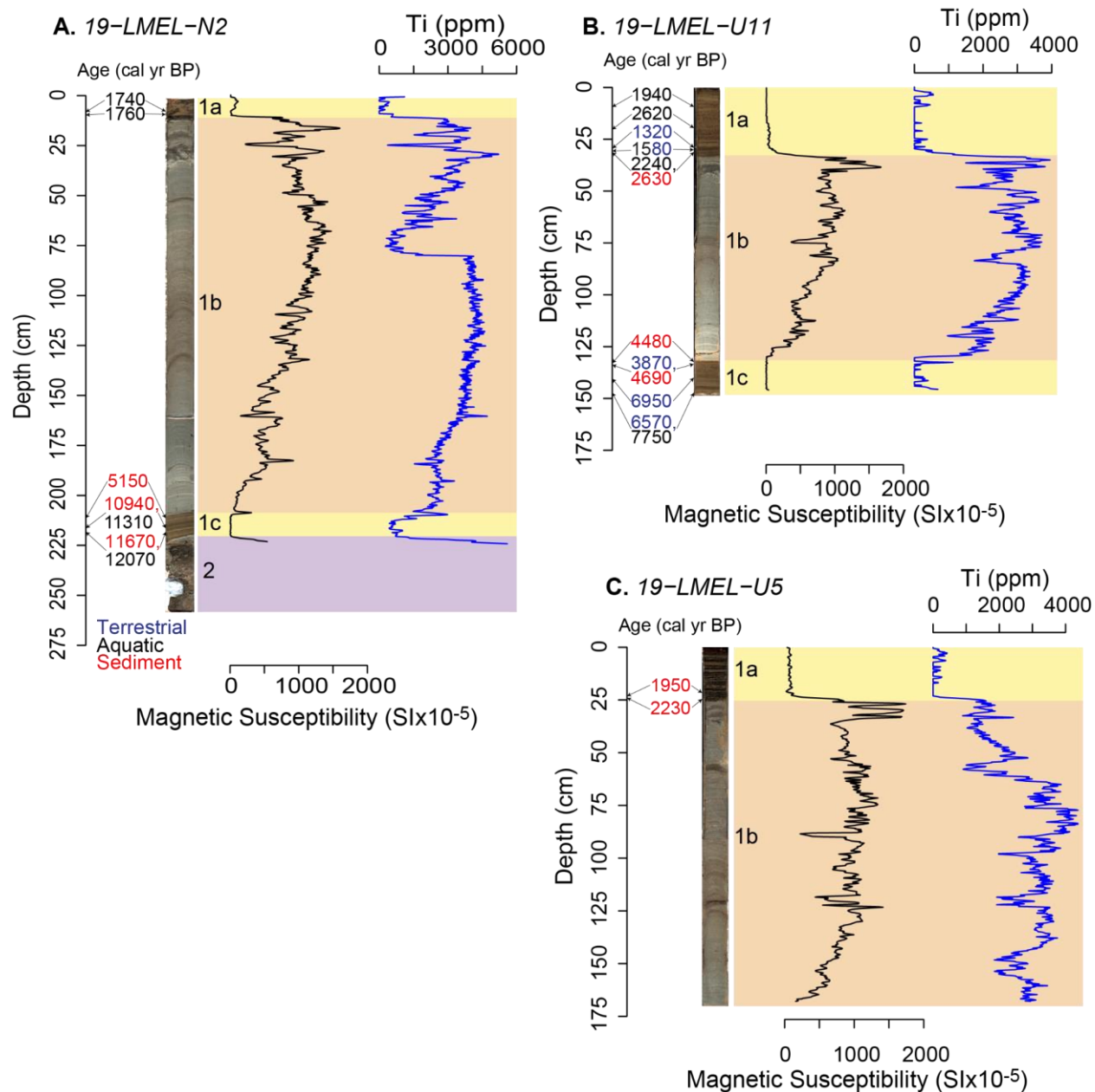
**Figure 2** Sediment core stratigraphy, sedimentary units, magnetic susceptibility (MS), and titanium abundance (Ti) for three cores from LMEL Lake. Numbers and arrows to the right of the depth axis indicate calibrated ages inferred from ^{14}C ages (terrestrial plant ages in blue, aquatic plant ages in black, and bulk sediment ages in red). Units are shown as colored and labeled rectangles to the right of each core image.

19-LMEL-U11 is 148.5 cm long and contains the three uppermost units contained within 19-LMEL-N2 (Fig. 2). Unit 1c (148.5-132 cm) is brown, laminated, organic, fine-grained sediment that contains terrestrial plant and aquatic moss remains, and has relatively low MS and Ti values. Unit 1b (132-34 cm) is gray, coarsely bedded to finely laminated silt/clay, contains no visible plant macrofossils, and has high MS and Ti concentrations. Unit 1a (34-0 cm) is very similar to Unit 1c, as it is

165    brown, contains terrestrial and aquatic plant remains, and returns to low MS and Ti values. This core has a well-preserved sediment-water interface.

19-LMEL-U5 is 169 cm long and has two units similar to the two uppermost units of 19-LMEL-N2 and 19-LMEL-U11 (Fig. 2). Unit 1b (169-25 cm) is gray, composed of silt/clay, and contains no obvious plant macrofossils. It has relatively high values of MS and Ti and the color also suggests low organic content. Unit 1a (0-25 cm) is brown, organic, fine-grained sediment with

170    many black laminations and has MS and Ti values close to zero. This unit contains few plant macrofossils, unlike Unit 1a in 19-LMEL-N2 and 19-LMEL-U11. The sediment-water interface is well preserved.

From the higher-elevation lake, core 19-UMEL-U2 is 91 cm long and contains two units (Fig. 3). Unit 2 (91-79 cm) of this core is similar to Unit 2 of 19-LMEL-N2, a gray diamicton with pebbles and granules in a matrix of silt/clay, with no visible organic materials or clear internal stratigraphy. The diamicton has relatively high values of MS and Ti. Unit 1 (79-0 cm) is

175    similar to Units 1a and 1c in the LMEL cores, as it is brown, organic, laminated, fine-grained sediment containing abundant aquatic moss remains, and has relatively low MS values and Ti concentrations. The sediment-water interface was slightly disturbed during coring.
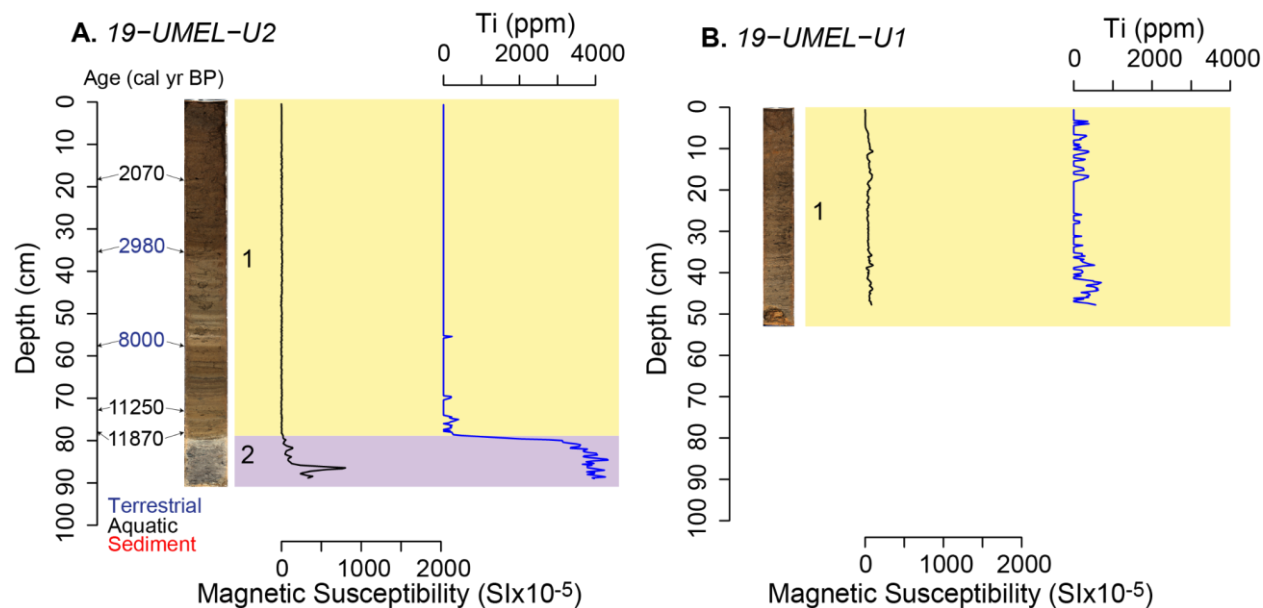
180    **Figure 3** Sediment core stratigraphy, units, MS, and Ti for two cores from UMEL Lake. Numbers and arrows to the right of the depth axis indicate calibrated ages. Numbers and arrows to the right of the depth axis indicate calibrated ages inferred from

[14]C ages (terrestrial plant ages in blue, aquatic plant ages in black, and bulk sediment ages in red). Colored and labeled rectangles to the right of the core image correspond to units.

185  19-UMEL-U1 is 53.5 cm long and contains only the lake's uppermost sedimentary unit (Fig. 3). Unit 1 is a brown, organic-rich fine-grained laminated sediment very similar to Unit 1 of 19-UMEL-U2 and Units 1a/1c of the LMEL cores.

**4.2 Sediment Core Chronology**

Radiocarbon sampling focused on constraining the ages of the sedimentary unit transitions described above. Due to the
190  infrequent occurrence of terrestrial plant macrofossils in the lake sediments, combined with the occurrence of potentially carbon-bearing metasedimentary bedrock and/or metasedimentary glacial drift in the lakes' watersheds, we dated multiple organic material types and aimed to assess reservoir effects on ^{14}C in aquatic moss and bulk organic materials. In all cases and across a range of time periods, terrestrial plant samples yielded younger apparent ages than aquatic moss or bulk sediment samples from the same depth (Fig. 4; Table 2). We argue that this reflects a reservoir effect, which is consistent with the
195  regional presence of metasedimentary rocks and causes aquatic moss and bulk sediment samples to appear older than they should. Thus, ages on aquatic mosses and bulk sediments are treated here as loose maximum estimates of depositional age, whereas ages on terrestrial plants provide tighter constraints on depositional age.
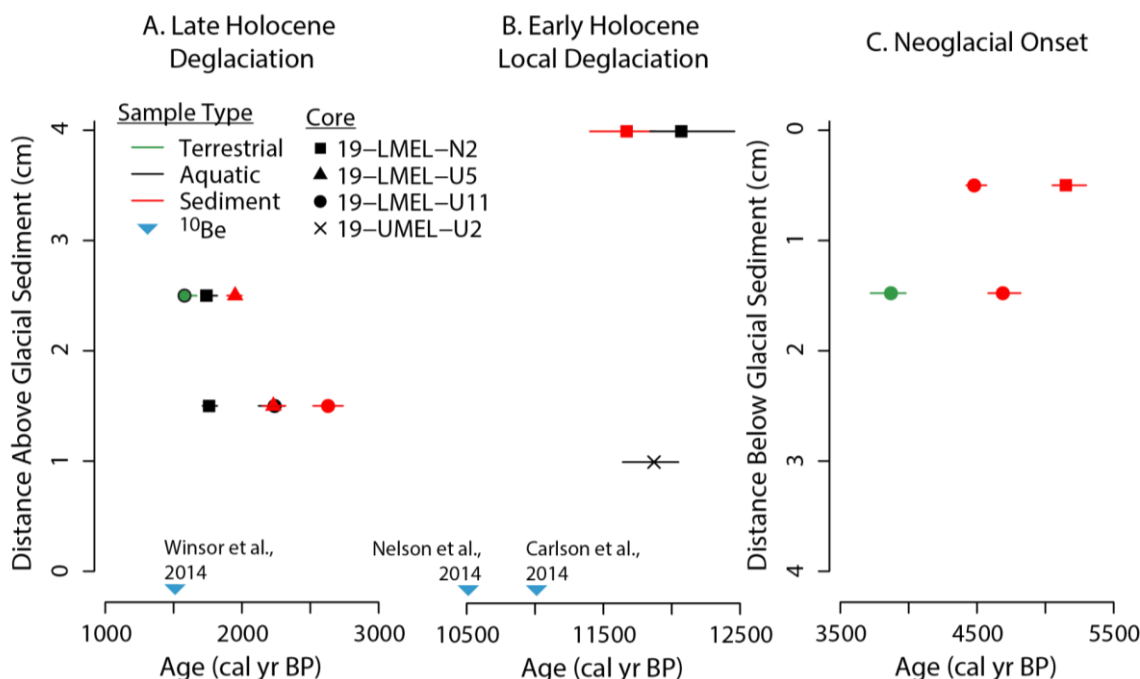
200  **Figure 4** Key radiocarbon ages near sedimentological transitions in four sediment cores from LMEL and UMEL. Note that ages from aquatic mosses (black) and bulk sediments (red) are presumed too old but provide loose maximum estimates of the

timing of organic matter deposition. (A) Ages from above inorganic, glaciolacustrine sediments that constrain the timing of late Holocene outlet glacier retreat (minimum limiting ages). (B) Ages from above glacial diamicton that constrain local deglaciation in the early Holocene (minimum limiting ages, but with hard water/reservoir effects from metasedimentary carbon sources to lake water). (C) Ages from below inorganic, glaciolacustrine sediments that constrain the timing of mid/late Holocene outlet glacier advance (maximum limiting ages).

The transition from diamicton to laminated sediments (from Unit 2 to Unit 1c in 19-LMEL-N2 and from Unit 2 to Unit 1 in 19-UMEL-U2) is constrained by ages of 12,070, 11,670, and 11,870 cal yr BP on two aquatic moss samples and one sediment sample from 1-4 cm above the transition (Fig. 4; Table 2). Stratigraphically, these are minimum limiting ages on the onset of laminated, organic sediment deposition (i.e. the inferred onset of lacustrine deposition), but because of the suspected reservoir effect these ages are likely at least several hundred years older than their actual timing of deposition so we do not treat them as such. Rather, these ages provide very loose estimates of timing. The transition from organic Unit 1c to inorganic Unit 1b in 19-LMEL-N2 and 19-LMEL-U11 likely occurred sometime after ~5200-3900 cal yr BP based on ^{14}C ages of one terrestrial plant sample and three sediment samples 1.5-0.5 cm below the transition (Fig. 4; Table 2). Finally, the most recent transition from inorganic Unit 1b to organic Unit 1a in all of the LMEL cores occurred sometime before ~1600 cal yr BP based on the ^{14}C age of one mixed terrestrial/aquatic plant sample, three aquatic moss samples, and three sediment samples from 2.5-1.5 cm above the transition (Fig. 4; Table 2).

## 5 Discussion

### 5.1 Interpretation of Sediments

We interpret the diamicton, Unit 2 in LMEL and UMEL (Figs. 2 and 3), as subglacial till deposited just prior to local deglaciation by the GrIS as the ice sheet retreated rapidly in the late glacial/early Holocene from its Last Glacial Maximum position beyond Greenland's modern-day coastline. Similar units are reported from other lakes in Greenland (e.g., Larsen et al., 2011). Unit 2 is only present in the longest core from each lake. Above the diamicton, both lakes contain fine-grained, laminated to bedded sediments (Unit 1c in LMEL and Unit 1 in UMEL) that we interpret as lacustrine. At the higher-elevation lake UMEL, Unit 1 is composed entirely of laminated, tan/brown organic-rich lake sediments with low MS and Ti values and abundant aquatic mosses (Fig. 3). We infer that UMEL sedimentation has not been influenced by glacier fluctuations since regional deglaciation. This system has maintained biologically productive, clear waters that support photosynthesis by aquatic mosses throughout the Holocene since regional deglaciation.

In contrast, Unit 1 of the lower-elevation lake LMEL contains both organic and inorganic lacustrine units (Fig. 2). Unit 1c is finely laminated, tan/brown organic sediments with relatively low Ti and MS values. This unit records establishment of a biologically productive lake with very little influx of mineral material following local deglaciation. Unit 1c is not recorded by 19-LMEL-U5 because it is the shortest core. Following the precedent of many past studies (Karlen and Matthews, 1992; Balascio et al., 2015; Adamson et al., 2022; Larocca and Axford, 2022), Unit 1b of 19-LMEL-N2, 19-LMEL-U11, and 19-

LMEL-U5 is interpreted as glaciolacustrine due to its relatively high MS and Ti values, gray color, silt/clay grain size, horizontal bedding, and absence of visible organic materials. Given the lake's setting, as described in the Study Area section above, glaciolacustrine deposition in LMEL is best explained by a late Holocene readvance of Kiattuut Sermiat. The outlet glacier thickened enough to enter the east-west valley that contains LMEL (Fig. 1C) and dammed the lake system's outlet

240     stream to create a large ice-marginal lake that subsumed LMEL. Above the glaciolacustrine sediments, Unit 1a of 19-LMEL-N2, 19-LMEL-U11, and 19-LMEL-U5 contains laminated, tan/brown, organic sediments with abundant aquatic mosses. This is interpreted as recording the retreat of Kiattuut Sermiat from its high lateral moraine in the late Holocene. This allowed the temporary, late Holocene proglacial lake to drain to an elevation below that of LMEL, which removed the glacial sediment source and enhanced biological production in LMEL. Differences in unit thickness between the three LMEL cores are

245     attributable to different sampling water depths and locations in the basin.

### 5.2 Local Greenland Ice Sheet Deglaciation

The transition from diamicton to organic lake sediments at LMEL and UMEL records local deglaciation by the GrIS. Minimum-limiting ^{14}C ages just above these transitions (1-4 cm above; N=3; Fig. 4; Table 2) suggest they occurred before

250     ~11,700 cal yr BP. In general, this is consistent with existing deglacial estimates from sites closer to the coast, where deglaciation happened earlier: ~14,800 cal yr BP at Nanortalik (Levy et al., 2020), ~13,600 cal yr BP from Lake N14 at the southern tip of Greenland (Björck et al., 2002; Puleo et al., 2022), ~13,400 cal yr BP at Pamiagdluk (Levy et al., 2020), and ~12,300 cal yr BP at Qaqortoq (Levy et al., 2020). However, our local deglaciation ages are earlier than suggested by [10]Be dates on boulders and bedrock near Kiattuut Sermiat and closest to our sites (~6.5 km southeast; Carlson et al., 2014; Nelson

255     et al., 2014). Carlson et al. (2014) suggest deglaciation between 11,100-10,600 cal yr BP and Nelson et al., 2014 suggest deglaciation at ~10,500 cal yr BP. This apparent discrepancy can be explained by the lake water reservoir effect we have identified on aquatic materials dated at LMEL and UMEL, and supports our assertion that terrestrial plant-based ^{14}C samples are most reliable in these lake sediments in a region where metasedimentary rocks are present. In 19-LMEL-U11, where paired terrestrial plant and bulk sediment based radiocarbon ages were evaluated at 133.5 cm depth (Table 2), the bulk sediment

260     radiocarbon sample appeared to be ~800 years older than the terrestrial plant radiocarbon sample. Tentatively using this offset would place our local deglaciation timing before ~10,900 cal yr BP, which is within the uncertainty of the nearby estimates (Larsen et al., 2011; Carlson et al., 2014; Nelson et al., 2014). It should be noted that this offset is not constant over time, thus we do not use it to present a precise estimate of local deglaciation. Our results contribute to an overall consensus that local deglaciation occurred between 11,100-10,500 cal yr BP around Narsarsuaq (Larsen et al., 2011; Carlson et al., 2014; Nelson

265     et al., 2014). Given that the demonstrated lake water ^{14}C reservoir effect at our sites can explain the discrepancy in local deglaciation timing, we argue the discrepancy is not due to small differences in elevation between the nearby [10]Be sampling sites (~560 m a.s.l.), other lake site (~600 m a.s.l.) and our lake sites (~670 m a.s.l.).

### 5.3 The Neoglacial Narsarsuaq Advance: Timing and Ice Surface Elevation

270    Kiattuut Sermiat's Holocene terminal moraine sits ~8 km outboard of its historic (Little Ice Age) end moraine system. [10]Be
       ages from the terminal moraine indicates it was abandoned ~1500 cal yr BP (Winsor et al., 2014). It has been suggested based
       on culmination timing that the corresponding advance occurred just before 2000 cal yr BP (Bennike and Sparrenbom, 2007),
       but the exact timing of advance is unknown. Lake sediment records hold a unique ability to reconstruct the timing of ice
       advance into watersheds in addition to retreat. We argue that the sedimentological transition from organic lacustrine Unit 1c

275    to inorganic lacustrine Unit 1b in LMEL cores (Fig. 2) records a Neoglacial readvance of Kiattuut Sermiat, which dammed the
       lake system's outlet stream and created a proglacial lake that encompassed LMEL. This readvance was not captured by the
       UMEL cores, indicating that the ice elevation was between the elevations of the two lakes. This new evidence from lake
       sediments is consistent with geomorphic evidence for a Holocene glacial advance that dammed the valley, including the large
       lateral moraine and shoreline features (Figs. 1D and E). Readvance extensive enough to dam the valley occurred sometime

280    after 3900 cal yr BP based on a terrestrial plant based ^{14}C sample 1.5 cm below the transition in 19-LMEL-U11 (Fig. 4; Table
       2). As discussed above, we believe terrestrial radiocarbon samples are the most reliable.

       Kiattuut Sermiat remained at a quite stable advanced position, damming, and feeding sediments into LMEL but not UMEL,
       from ~3900-1600 cal yr BP. The sediment cores from LMEL and UMEL provide unusually precise constraints on the thickness
       of Kiattuut Sermiat during that Neoglacial advance. LMEL (elev. ~670 m a.s.l.) cores contain glaciolacustrine sediments

285    recording the advance, while UMEL (elev. ~675 m a.s.l.) cores do not (Figs. 2 and 3). As described earlier, there is extensive
       geomorphic evidence for Kiattuut Sermiat entering the E-W valley that contains the lakes and creating a glacially dammed
       ice-marginal lake. Upon retreat after ~1600 cal yr BP, it left behind a moraine/dam. This moraine/dam has a modern elevation
       of ~580 m a.s.l. which is lower than the modern elevation of LMEL (~670 m a.s.l.), suggesting the lake that encompassed
       LMEL was ice-dammed. This ice-dammed lake would have filled the valley to the east of the moraine/dam roughly along the

290    670 m contour line on the modern landscape (Fig. 1C). The paleoshoreline features (Fig. 1E) indicate the lake reduced in size
       following the retreat of Kiattuut Sermiat and had its surface elevation set by the moraine at ~580 m a.s.l. This later version of
       the dammed lake did not contain modern LMEL or UMEL. This reveals that Kiattuut Sermiat had an ice surface elevation
       around ~670 m a.s.l. from ~3900-1600 cal yr BP at the location of the moraine/dam. This is ~250 m higher than the current
       ice elevation directly west of LMEL. Our elevation estimates do not account for glacial isostatic adjustment since subsequent

295    retreat; however, we suspect our estimate is within ~5 m of the true paleoglacier elevation. This is the difference in relative
       sea level change over the last 5000 years across south Greenland from Nanortalik to Qaqortoq (Sparrenbom et al., 2006;
       Sparrenbom et al., 2013).

       Readvance of Kiattuut Sermiat after 3900 cal yr BP adds to evidence for widespread Neoglacial advance (~4500-3000 cal yr
       BP) of outlet glaciers, mountain glaciers, and ice caps across much of the southern half of Greenland (Larocca and Axford,

300    2022). The closest existing sedimentary glacial reconstruction recording an advance in the mid/late Holocene is from Lower
       Nordbosø (~15 km northwest of LMEL/UMEL; Fig. 5a; Larsen et al., 2011). It records the readvance of GrIS outlet glaciers
       at ~3000 cal yr BP. Quvnerit Lake ~160 km southeast of LMEL/UMEL records a mountain glacier readvance at ~3100 cal yr

BP (Fig. 5a; Larocca et al., 2020a). Two smaller south Greenland mountain glacier systems studied by Larocca et al. (2020a) did not form until ~1300 cal yr BP, suggesting further cooling or wetter conditions at that time (Fig. 5a).

305
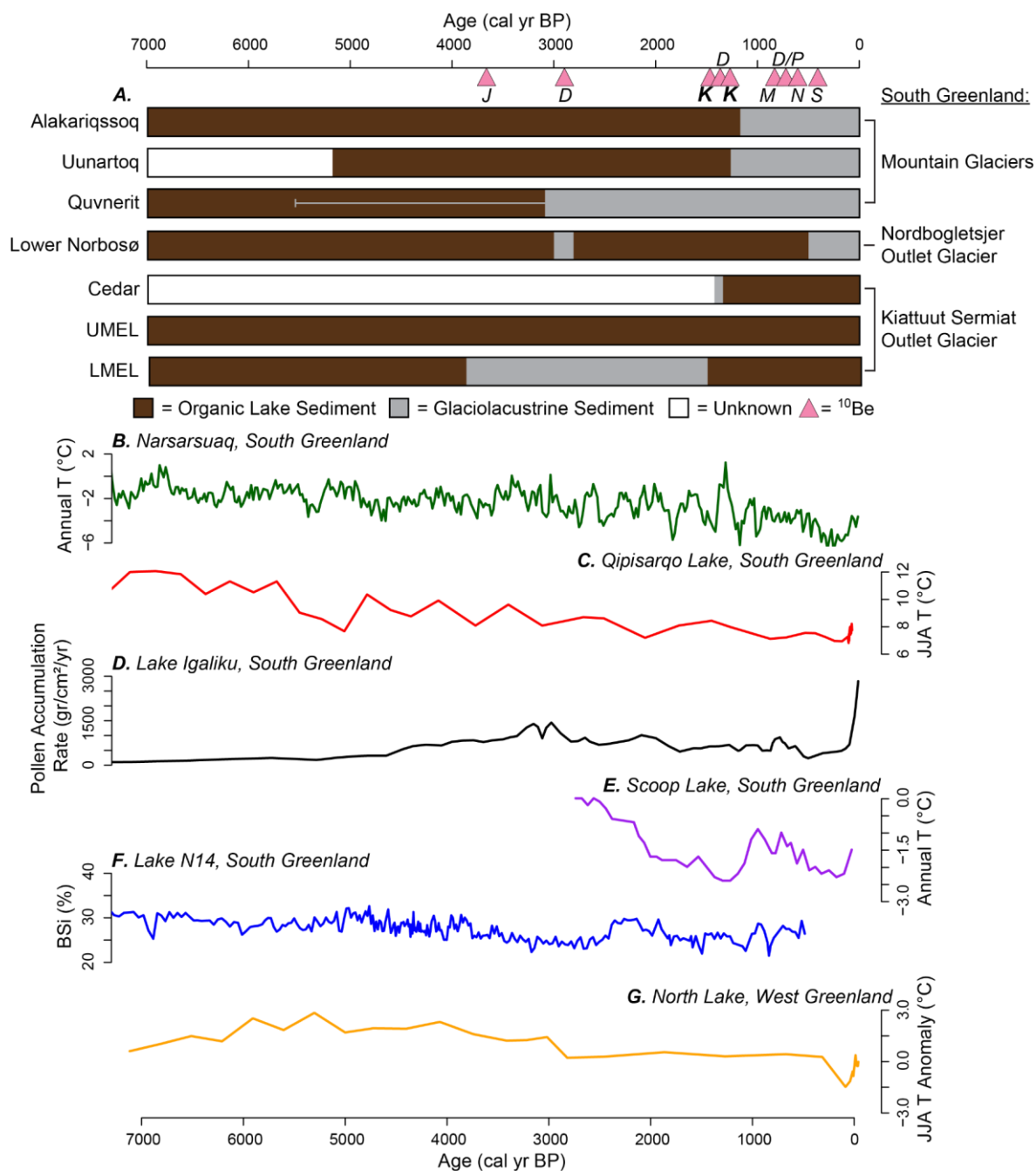
**Figure 5** Summary of LMEL/UMEL sediment core changes and regional paleoclimate records for the mid to late Holocene. (A) Periods of glaciolacustrine (gray) vs. non-glaciolacustrine (brown) lake sediments in south Greenland sediment cores. Alakariqssoq, Uunartoq, and Quvnerit lakes reflect local mountain glaciers (Larocca et al., 2020a). Lower Nordbosø sediments

310  reflect changes to Nordbogletsjer 15 km northwest of Kiattuut Sermiat (Larsen et al., 2011). Cedar Lake, LMEL, and UMEL sediments reflect Kiattuut Sermiat (Bennike and Sparrenbom, 2007; this study). Gray line (for Quvnerit) indicates times of reduced but detectable glacial input. Pink triangles indicate culmination timing from moraines in south Greenland. J=Jespersen Bræ (Sinclair, 2019), D=DV2L (Biette et al., 2021), K=Kiattuut Sermiat (Nelson et al., 2014; Winsor et al., 2014), M=Mosquito glacier (informal name; Sinclair et al., 2019), P=Paarlit Sermiat (Sinclair et al., 2019), N=Naajat Sermiat (Sinclair

315  et al., 2019), and S=Sermeq Kangilleq (Sinclair et al., 2019). (B) Annual temperature estimates for Narsarsuaq, South Greenland, based on Summit, Greenland, ice core $\delta^{15}N$ values combined with a climate model (Buizert et al., 2018). (C) Summer air temperatures inferred from pollen assemblages at Qipisarqo Lake (Fréchette and de Vernal, 2009). (D) Annual pollen grain accumulation rates at Lake Igaliku (Massa et al., 2012). (E) Chironomid head capsule oxygen isotope inferred annual air temperatures at Scoop Lake (Lasher and Axford, 2019). (F) Percent biogenic silica at Lake N14 (Andresen et al.,

320  2004). (G) Chironomid assemblage based summer air temperature anomalies relative to present at North Lake in western Greenland (Axford et al., 2013).

[10]Be ages from the outermost Holocene moraine deposited by Jespersen Bræ, which drains the Julianehåb Ice Cap (~25 km east/southeast of LMEL/UMEL), indicates a late Holocene culmination at ~3700 cal yr BP (Fig. 5a; Sinclair, 2019). An

325  additional set of [10]Be samples from the outermost moraines deposited by the DV2L mountain glacier (~50 km southeast of LMEL/UMEL) indicates a culmination age of ~2900 cal yr BP (Fig. 5a; Biette et al., 2021). These culmination ages imply mid/late Holocene glacier advances followed by retreat at these times. Many other outermost moraines record younger late Holocene culmination ages in south Greenland (Sinclair, 2019; Biette et al., 2021), but this could be due to later glacial advances destroying moraines deposited in prior Neoglacial advances. The majority of records that can address the Neoglacial

330  advance in south Greenland indicate it occurred between ~4000-3000 cal yr BP.

Farther afield in southeast Greenland, Kulusuk Lake indicates a mountain glacier advanced at 4100, 3900, and 3200 cal yr BP (~630 km northeast of LMEL/UMEL; Balascio et al., 2015). 60 km north of Kulusuk Lake, [10]Be ages from outermost moraines deposited by the TAS-A and TAS-B mountain glaciers have culmination ages at ~3300 and ~3750 cal yr BP, respectively (Biette et al., 2021). This evidence suggests a similar timing for Neoglacial advance in southeast Greenland (~4000-3000 cal

335  yr BP).

In southwest Greenland, Lake 09370 records an advance of a GrIS outlet glacier at ~3700 cal yr BP (~290 km northwest of LMEL/UMEL; Larsen et al., 2015). Four other southwest Greenland lakes that received glacial meltwater from GrIS outlet glaciers at some point in their past did not record a Neoglacial advance (Larsen et al., 2015). Langesø Lake and Badesø Lake of southwest Greenland record advances of local mountain glaciers into their catchments at ~3600 and ~3500 cal yr BP,

340  respectively (~450 km northwest of LMEL/UMEL; Larsen et al., 2017). The third reconstruction presented by Larsen et al.

(2017) from Lake IS21 did not record a Neoglacial advance of a local ice cap. Crash Lake of southwest Greenland records an overall trend of advancing Sukkertoppen glaciers and ice caps after ~4600 cal yr BP with centennial scale variations (Schweinsberg et al., 2018). Pers Lake of southwest Greenland records small glacial meltwater inputs beginning at ~4300 cal yr BP indicating the growth of nearby mountain glaciers (Larocca et al., 2020b). Overall, evidence from this region appears

345    more mixed, with several outlet glacier reconstructions showing no signs of a Neoglacial advance. This could be explained by the greater climate sensitivity of mountain glaciers compared to outlet glaciers and ice caps and/or the glacial advances not reaching the watersheds of the sampled threshold lakes. Regardless, it appears that the Neoglacial readvance was registered slightly earlier in southwest Greenland, from ~4500-3500 cal yr BP. Finally, in west Greenland, Sikuiui Lake captured ice cap growth at 5000 cal yr BP, with further glacial expansion at ~3700 cal yr BP (~1040 km north/northwest of LMEL/UMEL;

350    Schweinsberg et al., 2017).

Paleoclimate records from south Greenland support that glacial advances were driven by regional cooling between ~4500-3000 cal yr BP. Pollen assemblages from Qipisarqo Lake (~130 km west of LMEL/UMEL) suggest July surface air temperatures cooled at a rate of 0.5°C per 1,000 years over the last ~7,000 years (Fig. 5c; Fréchette and de Vernal, 2009). Another temperature record from Qipisarqo Lake based on chironomid head capsule oxygen isotope values finds similar

355    results, with mean annual temperatures decreasing ~4°C from 8300 cal yr BP to present (Wooller et al., 2004). A third record from Qipisarqo Lake suggests the onset of Neoglacial cooling occurred at ~3000 cal yr BP based on decreasing biogenic silica and organic content of the sediment (Kaplan et al., 2002). Pollen assemblages from Lake Igaliku (~30 km south of LMEL/UMEL) indicate that moister and cooler conditions began at ~4700 cal yr BP and pollen assemblages and accumulation rates suggest cooling was enhanced after 3000 cal yr BP (Fig. 5d; Massa et al., 2012). At Scoop Lake (~60 km south of

360    LMEL/UMEL), Neoglacial cooling of ~2°C occurred from ~3000-1500 cal yr BP based on a chironomid oxygen isotope reconstruction (Fig. 5e; Lasher and Axford, 2019). A reconstruction of biogenic silica and minerogenic content of sediment from Lake N14 at the southern tip of Greenland indicates that cooling likely began at ~4700 cal yr BP with enhanced cooling after ~3700 cal yr BP (Fig. 5f; Andresen et al., 2004). Farther away, near Ilulissat in west Greenland (~920 km northwest of LMEL/UMEL), a chironomid assemblage based temperature reconstruction from North Lake reconstructs a summer cooling

365    of 2-3°C from ~4000-200 cal yr BP (Fig. 5g; Axford et al., 2013).

Marine records near south Greenland also indicate Neoglacial cooling and/or glacial advance. A marine sediment core (PO 243-451) from the Igaliku Fjord of south Greenland indicates cool and stratified water-column conditions at ~3200-2800 cal yr BP and ~2600-2300 cal yr BP based on foraminifera species (Lassen et al., 2004). Another marine sediment record from the Narsaq Sound of south Greenland suggests Neoglaciation began at ~4800 cal yr BP due to ice rafted debris peaks at 4600

370    and 3600 cal yr BP (Nørgaard-Pedersen and Mikkelsen, 2009). A marine core from the Ameralik Fjord of southwest Greenland indicates the onset of Neoglaciation at ~3200 cal yr BP based on foraminifera species (Seidenkrantz et al., 2007). Just off the coast of southeast Greenland, a multiproxy record developed on core JM96-1206/2GC suggests the East Greenland Current, which carries cold Arctic water to south Greenland, strengthened and forced the relatively warm, Atlantic-sourced Irminger Current water to the subsurface during the Neoglacial beginning at ~4500 cal yr BP (Perner et al., 2016).

375    In summary, evidence indicates that a cooling-driven advance of many GrIS outlet glaciers, mountain glaciers, and ice caps in
the southern sectors of Greenland occurred between ~4500-3000 cal yr BP and our record adds to that evidence. The main
drivers of overall cooling through the mid/late Holocene in south Greenland were decreasing Northern Hemisphere summer
insolation (Berger and Loutre, 1999) and increased delivery of cold, Arctic waters via the strengthening East Greenland Current
(Perner et al., 2016).

380

**5.4 Late Holocene Retreat from the Narsarsuaq Moraine**

All LMEL sediment cores record a transition from minerogenic, glaciolacustrine sediment (Unit 1b) to organic lake sediments
(Unit 1a) which represents a local retreat of Kiattuut Sermiat in the late Holocene (Fig. 2a). One mixed terrestrial and aquatic
plant radiocarbon sample 2.5 cm above the transition indicates that this retreat from the watershed occurred near or just prior

385    to ~1600 cal yr BP, and related ages from aquatic plants or bulk sediments support this age though they presumably reflect
large reservoir effects (Fig. 4; Table 2). We cannot definitively say that retreat occurred before ~1600 cal yr BP, as aquatic
organic materials at LMEL are subject to a reservoir effect and likely reflect ages that are too old.

Nonetheless, this age constraint is consistent with reconstructions from the terminus of Kiattuut Sermiat that indicate the outlet
glacier retreated between ~1600-1300 cal yr BP. At Cedar Lake, which is ~13 km southwest of LMEL/UMEL and within the

390    outermost moraines deposited by Kiattuut Sermiat, terrestrial plant based radiocarbon samples from just above the minerogenic
to organic lake sediment transition indicate Kiattuut Sermiat retreated prior to ~1300 cal yr BP (Fig. 5a; Bennike and
Sparrenbom, 2007). Winsor et al. (2014) reported several [10]Be samples from the outermost moraines deposited by Kiattuut
Sermiat with a mean age of ~1500 cal yr BP, indicating the culmination timing of the largest advance of this outlet glacier
(Fig. 5a). Another [10]Be sample from a boulder downstream of Kiattuut Sermiat also indicated culmination at ~1500 cal yr BP

395    (Nelson et al., 2014).

Retreat of Kiattuut Sermiat at ~1500 cal yr BP contrasts conspicuously with the strong evidence for regional cooling at this
time, and with the majority of published glacier reconstructions from the region. Nearby, Lower Nordbosø sediment indicates
a GrIS outlet glacier retreated from its catchment at ~2800 cal yr BP and remained out of the catchment until 500 cal yr BP
(Fig. 5a; Larsen et al., 2011). Quvnerit Lake, Alakariqssoq Lake, and Uunartoq Lake of south Greenland record the constant

400    presence of mountain glaciers in their watersheds from 3100 cal yr BP to present, 1300 cal yr BP to present, and 1200 cal yr
BP to present, respectively (Fig. 5a; Larocca al., 2020a). An outermost moraine deposited by Naajat Sermiat (GrIS outlet
glacier; ~75 km west/southwest of LMEL/UMEL) of south Greenland has been dated to ~600 cal yr BP (Fig. 5a; Sinclair,
2019). A south Greenland moraine formed by Sermeq Kangilleq (Julianehåb Ice Cap outlet glacier; 40 km southeast of
LMEL/UMEL) has been [10]Be sampled and dated to ~400 cal yr BP (Fig. 5a; Sinclair, 2019). Paarlit Sermiat, an outlet glacier

405    draining an unnamed ice cap ~125 km southeast of LMEL/UMEL, deposited a moraine at ~700 cal yr BP based on [10]Be ages
(Fig. 5a; Sinclair, 2019). A mountain glacier (Mosquito Glacier; ~110 km southeast of LMEL/UMEL) moraine stabilized at
~800 cal yr BP (Fig. 5a; Sinclair, 2019). One moraine was deposited by the DV2L mountain glacier of south Greenland at

~1400 cal yr BP based on [10]Be samples (Biette et al., 2021). This final moraine [10]Be age is the only other evidence from south Greenland indicating a culmination and retreat timing of an outermost moraine around ~1500 cal yr BP.

410 In southeast Greenland, only one [10]Be dated moraine shows a similar culmination timing to Kiattuut Sermiat at around 1500 cal yr BP (Biette et al., 2021). The remaining lake sediment (Balascio et al., 2015) and moraine (Biette et al., 2021) based glacial reconstructions from this region show no sign of retreat at this time. A larger number of lake sediment based glacial reconstructions exist in southwest Greenland and show mixed evidence. Three lake records show outlet glacier and ice cap retreat within a few hundred years of Kiattuut Sermiat's retreat including 09370 Lake (Larsen et al., 2015), Frederikshåb

415 Isblink (Larsen et al., 2015), and Lake IS21 (Larsen et al., 2017). However, each of these records also shows an advance of equal or larger magnitude occurring in the past millennium, unlike Kiattuut Sermiat. Several other records show no sign of retreat around 1500 cal yr BP, including Kan01 Lake (Larsen et al., 2015), Langesø Lake (Larsen et al., 2017), Badesø Lake (Larsen et al., 2017), Crash Lake (Schweinsberg et al., 2018), and Pers Lake (Larocca et al., 2020a).

Climate records from the southern half of Greenland show an overall cooling trend through the mid/late Holocene with some

420 showing a brief period of warming during the Medieval Climate Anomaly before cooling again during the Little Ice Age (Fig. 5B-G; Kaplan et al., 2002; Andresen et al., 2004; Wooller et al., 2004; Fréchette and de Vernal, 2009; Massa et al., 2012; Axford et al., 2013; Buizert et al., 2018; Lasher and Axford, 2019). Nearby marine records corroborate a cooling trend in the late Holocene with warming during the Medieval Climate Anomaly followed by cooling during the Little Ice Age (Lassen et al., 2004; Seidenkrantz et al., 2007; Nørgaard-Pedersen and Mikkelsen, 2009). This late Holocene cooling drove glacial

425 advances across Greenland, presumably including Kiattuut Sermiat. However, warming during the Medieval Climate Anomaly appears too late to be the driver of Kiattuut Sermiat's late Holocene retreat. Rather than temperature, the retreat of Kiattuut Sermiat at ~1500 cal yr BP could potentially be driven by differing precipitation amounts. Late Holocene precipitation amount reconstructions from Greenland are limited to relatively high elevation ice core sites and reflect variable conditions (Cuffey and Clow, 1997; Badgeley et al., 2020; Osman et al., 2021). Because of this, it is unclear if a local precipitation reduction

430 could have potentially driven Kiattuut Sermiat retreat. Another potential factor is that Kiattuut Sermiat is located where the GrIS meets the Julianehåb Ice Cap and where passive ice margins meet fast-flowing outlet glaciers (Larsen et al., 2011). This local glaciological complexity in combination with any local precipitation reduction could potentially account for the unusual timing and magnitude of Kiattuut Sermiat's late Holocene retreat.

Another unusual, although not unique, feature of Kiattuut Sermiat's history is that its advance during the Little Ice Age was

435 notably lesser than the earlier Neoglacial Narsarsuaq advance. We find that Kiattuut Sermiat did not readvance into the LMEL or UMEL watersheds during the Little Ice Age, consistent with the location of the glacier's Little Ice Age moraines just outboard of the modern glacier terminus (Winsor et al., 2015). This is unlike the response of many other glaciers in Greenland that deposited their outermost late Holocene moraines during the Little Ice Age (Kelly and Funder, 2009; Kjær et al., 2022). Little Ice Age glacier maxima are consistent with widespread evidence that progressive insolation-driven cooling made the

440 last millennium the coldest period of the middle to late Holocene across much of Greenland and the Arctic (Kaufman et al., 2009; Briner et al., 2016). During the Little Ice Age, GISP2, DYE3, and Nuussuaq ice cores all suggest lower precipitation

amounts than present (Cuffey and Clow, 1997; Badgeley et al., 2020; Osman et al., 2021) which could indicate Kiattuut Sermiat is highly sensitive to changes in precipitation given its limited advance compared to other nearby south Greenland outlet glaciers (Larsen et al., 2011).

445

## 6 Conclusions

Sedimentary records from two adjacent upland lakes substantially improve our understanding of the late Holocene history of a GrIS outlet glacier. In particular, we reconstruct the timing and thickness of the major Neoglacial advance of Kiattuut Sermiat, and confirm the timing of its subsequent late Holocene retreat. Our ^{14}C-based age constraint on regional deglaciation

450  timing (~11,700 cal yr BP) is slightly older than the timing from [10]Be samples around Narsarsuaq (~11,000 cal yr BP), likely due to a reservoir effect in aquatic plant radiocarbon samples. We find that the Neoglacial advance of Kiattuut Sermiat that deposited the Narsarsuaq end moraines dammed a tributary ice-marginal upland valley, creating an ice-dammed lake. The temporary ice-dammed lake subsumed one of our study lakes, LMEL, after ~3900 cal yr BP. The slightly higher-elevation adjacent lake, UMEL, remained outside the limits of the ice-dammed lake, indicating an ice dam elevation of ~670 m. This

455  advance was driven by regional cooling that led to the advance of many Greenland glaciers between ~4500-3000 cal yr BP. The ice dammed lake and thickness of Kiattuut Sermiat was maintained at ~670 m until ~1600 cal yr BP, when LMEL sediments show a transition back to organic, non-glacier influenced lake sediments for the remainder of the record. This retreat does not appear to have been driven by local or regional warming, but instead may have been caused by changes in precipitation amounts and/or related to the glaciological complexity of this particular outlet glacier, which is influenced by the Julianehåb

460  Ice Cap adjacent to the GrIS. In the future, high-resolution ice sheet models could be used to further determine what factors drove Kiattuut Sermiat retreat at this time, and what explained the relatively small magnitude of this outlet glacier's Little Ice Age advance compared with the extensive late Holocene Narsarsuaq advance.

### Data Availability

465  The LMEL and UMEL radiocarbon, Magnetic Susceptibility, and titanium concentration data are available on the NOAA paleoclimate data center: https://www.ncei.noaa.gov/access/paleo-search/study/37700.

### Supplement

The supplement related to this article is available online at:

470

### Author Contributions

PP contributed to funding acquisition, field work, laboratory work, formal analysis, visualization, data curation, writing of the draft manuscript, review of the draft manuscript. YA contributed to conceptualization, funding acquisition, project administration, resources, supervision, writing of the draft manuscript, and review of the draft manuscript.

475

**Competing Interests**

The authors declare that they have no conflict of interest.

**Acknowledgements**

480    We thank Grace Schellinger, Mia Tuccillo, Bailey Nash, and Aidan Burdick for assistance with lab work. Additional thanks
go to Laura Larocca, G. Everett Lasher, Tim Coston, Aaron Hartz, Polar Field Services, the U.S. Air National Guard, Blue Ice
Explorer, and Air Greenland for assistance during field work. We also thank Sarah Woodroffe for helpful discussions regarding
isostasy. We are appreciative of the Woods Hole Oceanographic Institution - National Ocean Sciences Accelerator Mass
Spectrometry facility and Beta Analytic for radiocarbon analysis. We are grateful to the people and Government of Greenland

485    for allowing us to work on their land. Samples were collected with permission of the Government of Greenland's
(Naalakkersuisut) scientific survey license VU-00160 and minerals export permit 025/2019. DEMs were provided by the Polar
Geospatial Center under NSF-OPP awards 1043681, 1559691, and 1542736.

**Financial Support**

490    This work was supported financially by NSF OPP awards 1454734 and 2002515 to Yarrow Axford and an NSF Graduate
Research Fellowship to Peter Puleo.

**References**

495    Adamson, K., Lane, T., Carney, M., Delaney, C., Howden, A.: The imprint of catchment processes on Greenlandic ice cap
proglacial lake records: analytical approaches and palaeoenvironmental significance. Journal of Quaternary Science 37, 1388-
1406, 2022.

Andresen, C.S., Björck, S., Bennike, O., Bond, G.: Holocene climate changes in southern Greenland: evidence from lake
sediments. Journal of Quaternary Science 19, 783-795, 2004.

500    Axford, Y., De Vernal, A., Osterberg, E.C.: Past Warmth and Its Impacts During the Holocene Thermal Maximum in
Greenland. Annual Review of Earth and Planetary Sciences 49, 279-307, 2021.

Axford, Y., Losee, S., Briner, J.P., Francis, D.R., Langdon, P.G., Walker, I.R.: Holocene temperature history at the western
Greenland Ice Sheet margin reconstructed from lake sediments. Quaternary Science Reviews 59, 87-100, 2013.

Badgeley, J.A., Steig, E.J., Hakim, G.J., Fudge, T.J.: Greenland temperature and precipitation over the last 20 000 years using
505    data assimilation. Climate of the Past 16, 1325-1346, 2020.

Balascio, N.L., amp, apos, Andrea, W.J., Bradley, R.S.: Glacier response to North Atlantic climate variability during the Holocene. Climate of the Past 11, 1587-1598, 2015.

Bennike, O., Sparrenbom, C.J.: Dating of the Narssarssuaq stade in southern Greenland. The Holocene 17, 279-282, 2007.

Berger, A., Loutre, M.F.: Insolation Values for the Climate of the Last 10 Million Years. Quaternary Science Reviews 10, 297-317, 1999.

Biette, M., Jomelli, V., Chenet, M., Braucher, R., Menviel, L., Swingedouw, D., Rinterknecht, V.: Evidence of the largest Late Holocene mountain glacier extent in southern and southeastern Greenland during the middle Neoglacial from [10]Be moraine dating. Boreas, 1-17, 2021.

Bjørk, A.A., Kruse, L.M., Michaelsen, P.B.: Brief communication: Getting Greenland's glaciers right – a new data set of all official Greenlandic glacier names. The Cryosphere 9, 2215-2218, 2015.

Björck, S., Bennike, O., Rosén, P., Andresen, C.S., Bohncke, S., Kaas, E., Conley, D.J.: Anomalously mild Younger Dryas summer conditions in southern Greenland. Geology 30, 427-430, 2002.

Briner, J.P., McKay, N.P., Axford, Y., Bennike, O., Bradley, R.S., de Vernal, A., Fisher, D., Francus, P., Fréchette, B., Gajewski, K., Jennings, A., Kaufman, D.S., Miller, G., Rouston, C., Wagner, B.: Holocene climate change in Arctic Canada and Greenland. Quaternary Science Reviews 147, 340-364, 2016.

Buizert, C., Keisling, B.A., Box, J.E., He, F., Carlson, A.E., Sinclair, G., DeConto, R.M.: Greenland-Wide Seasonal Temperatures During the Last Deglaciation. Geophysical Research Letters 45, 1905-1914, 2018.

Cappelen, J.: Climatological Standard Normals 1981-2010 - Denmark, The Faroe Islands and Greenland - Based on Data Published in DMI Reports 18-02, 18-04 and 18-05. DMI Report 18-19, DMI, Copenhagen, 2019.

Carlson, A.E., Winsor, K., Ullman, D.J., Brook, E.J., Rood, D.H., Axford, Y., LeGrande, A.N., Anslow, F.S., Sinclair, G.: Earliest Holocene south Greenland ice sheet retreat within its late Holocene extent. Geophysical Research Letters 41, 5514-5521, 2014.

Cuffey, K.M., Clow, G.D.: Temperature, accumulation, and ice sheet elevation in central Greenland through the last deglacial transition. Journal of Geophysical Research: Oceans 102, 26383-26396, 1997.

Dowdeswell, J.A.: Atmospheric science. The Greenland Ice Sheet and global sea-level rise. Science 311, 963-964, 2006.

Fréchette, B., De Vernal, A.: Relationship between Holocene climate variations over southern Greenland and eastern Baffin Island and synoptic circulation pattern. Climate Past 5, 347-359, 2009.

Goelzer, H., Nowicki, S., Payne, A., Larour, E., Seroussi, H., Lipscomb, W.H., Gregory, J., Abe-Ouchi, A., Shepherd, A., Simon, E., Agosta, C., Alexander, P., Aschwanden, A., Barthel, A., Calov, R., Chambers, C., Choi, Y., Cuzzone, J., Dumas,
535    C., Edwards, T., Felikson, D., Fettweis, X., Golledge, N.R., Greve, R., Humbert, A., Huybrechts, P., Le clec'h, S., Lee, V., Leguy, G., Little, C., Lowry, D.P., Morlighem, M., Nias, I., Quiquet, A., Rückamp, M., Schlegel, N.-J., Slater, D.A., Smith, R.S., Straneo, F., Tarasov, L., van de Wal, R., van den Broeke, M.: The future sea-level contribution of the Greenland ice sheet: a multi-model ensemble study of ISMIP6. The Cryosphere 14, 3071-3096, 2020.

Greve, R., Chambers, C.: Mass loss of the Greenland ice sheet until the year 3000 under a sustained late-21st-century climate.
540    Journal of Glaciology 68, 618-624, 2022.

Kaplan, M.R., Wolfe, A.P., Miller, G.H.: Holocene Environmental Variability in Southern Greenland Inferred from Lake Sediments. Quaternary Research 58, 149-159, 2002.

Karlen, W., Matthews, J.A.: Reconstructing Holocene Glacier Variations from Glacial Lake Sediments: Studies from Nordvestlandet and Jostedalsbreen-Jotunheimen, Southern Norway. Geogr Ann A 74, 327-348, 1992.

545    Kaufman, D.S., Schneider, D.P., McKay, N.P., Ammann, C.M., Bradley, R.S., Briffa, K.R., Miller, G.H., Otto-Bliesner, B.L., Overpeck, J.T., Vinther, B.M., Arctic Lakes 2k Project Members: Recent warming reverses long-term arctic cooling. Science 325, 1236-1239, 2009.

Kelly, M.A., Lowell, T.V.: Fluctuations of local glaciers in Greenland during latest Pleistocene and Holocene time. Quaternary Science Reviews 28, 2088-2106, 2009.

550    Kjær, K.H., Bjørk, A.A., Kjeldsen, K.K., Hansen, E.S., Andresen, C.S., Siggaard-Andersen, M.-L., Khan, S.A., Søndergaard, A.S., Colgan, W., Schomacker, A., Woodroffe, S., Funder, S., Rouillard, A., Jensen, J.F., Larsen, N.K.: Glacier response to the Little Ice Age during the Neoglacial cooling in Greenland. Earth-Science Reviews 227, 1-43, 2022.

Larocca, L.J., Axford, Y.: Arctic glaciers and ice caps through the Holocene:a circumpolar synthesis of lake-based reconstructions. Climate of the Past 18, 579-606, 2022.

555    Larocca, L.J., Axford, Y., Bjørk, A.A., Lasher, G.E., Brooks, J.P.: Local glaciers record delayed peak Holocene warmth in south Greenland. Quaternary Science Reviews 241, 106421, 1-16, 2020a.

Larocca, L.J., Axford, Y., Woodroffe, S.A., Lasher, G.E., Gawin, B.: Holocene glacier and ice cap fluctuations in southwest Greenland inferred from two lake records. Quaternary Science Reviews 246, 2020b.

Larsen, N.K., Kjær, K.H., Lecavalier, B., Bjørk, A.A., Colding, S., Huybrechts, P., Jakobsen, K.E., Kjeldsen, K.K., Knudsen, K.-L., Odgaard, B.V., Olsen, J.: The response of the southern Greenland ice sheet to the Holocene thermal maximum. Geology 43, 291-294, 2015.

Larsen, N.K., Kjær, K.H., Olsen, J., Funder, S., Kjeldsen, K.K., Nørgaard-Pedersen, N.: Restricted impact of Holocene climate variations on the southern Greenland Ice Sheet. Quaternary Science Reviews 30, 3171-3180, 2011.

Larsen, N.K., Strunk, A., Levy, L.B., Olsen, J., Bjørk, A., Lauridsen, T.L., Jeppesen, E., Davidson, T.A.: Strong altitudinal control on the response of local glaciers to Holocene climate change in southwest Greenland. Quaternary Science Reviews 168, 69-78, 2017.

Lasher, G.E., Axford, Y.: Medieval warmth confirmed at the Norse Eastern Settlement in Greenland. Geology 47, 267-270, 2019.

Lassen, S.J., Kuijpers, A., Kunzendorf, H., Hoffmann-Wieck, G., Mikkelsen, N., Konradi, P.: Late-Holocene Atlantic bottom-water variability in Igaliku Fjord, South Greenland, reconstructed from foraminifera faunas. The Holocene 14, 165-171, 2004.

Levy, L.B., Larsen, N.K., Knudsen, M.F., Egholm, D.L., Bjørk, A.A., Kjeldsen, K.K., Kelly, M.A., Howley, J.A., Olsen, J., Tikhomirov, D., Zimmerman, S.R.H., Kjær, K.H.: Multi-phased deglaciation of south and southeast Greenland controlled by climate and topographic setting. Quaternary Science Reviews 242, 1-12, 2020.

Massa, C., Perren, B.B., Gauthier, É., Bichet, V., Petit, C., Richard, H.: A multiproxy evaluation of Holocene environmental change from Lake Igaliku, South Greenland. Journal of Paleolimnology 48, 241-258, 2012.

Monnin, E., Indermuhle, A., Dallenbach, A., Fluckiger, J., Stauffer, B., Stocker, T.F., Raynaud, D., Barnola, J.M.: Atmospheric $CO_2$ concentrations over the last glacial termination. Science 291, 112-114, 2001.

Nelson, A.H., Bierman, P.R., Shakun, J.D., Rood, D.H.: Using in situ cosmogenic $^{10}$Be to identify the source of sediment leaving Greenland. Earth Surface Processes and Landforms 39, 1087-1100, 2014.

Nesje, A.: A Piston Corer for Lacustrine and Marine-Sediments. Arctic and Alpine Research 24, 257-259, 1992.

Nørgaard-Pedersen, N., Mikkelsen, N.: 8000 year marine record of climate variability and fjord dynamics from Southern Greenland. Marine Geology 264, 177-189, 2009.

Oerlemans, J.: Glaciers and Climate Change. Balkema, Lisse, 2001.

Osman, M.B., Smith, B.E., Trusel, L.D., Das, S.B., McConnell, J.R., Chellman, N., Arienzo, M., Sodemann, H.: Abrupt
585   Common Era hydroclimate shifts drive west Greenland ice cap change. Nature Geoscience 14, 756-761, 2021.

Perner, K., Jennings, A.E., Moros, M., Andrews, J.T., Wacker, L.: Interaction between warm Atlantic-sourced waters and the
East Greenland Current in northern Denmark Strait (68°N) during the last 10 600 cal a BP. Journal of Quaternary Science 31,
472-483, 2016.

Porter, C., Morin, P., Howat, I., Noh, M.J., Bates, B., Peterman, K., Keesey, S., Schlenk, M., Gardiner, J., Tomko, K., Willis,
590   M., Kelleher, C., Cloutier, M., Husby, E., Foga, S., Nakamura, H., Platson, M., Wethington, M., Williamson, C., Bauer, G.,
Enos, J., Arnold, G., Kramer, W., Becker, P., Doshi, A., D'Souza, C., Cummens, P., Laurier, F., Bojesen, M.: ArcticDEM,
Harvard Dataverse V1, https://doi.org/10.7910/DVN/OHHUKH, 2018.

Puleo, P.J.K., Masterson, A.L., Medeiros, A.S., Schellinger, G., Steigleder, R., Woodroffe, S., Osburn, M.R., Axford, Y.:
Younger Dryas and early Holocene climate in south Greenland inferred from oxygen isotopes of chironomids, aquatic Moss,
595   and Moss cellulose. Quaternary Science Reviews 296, 1-16, 2022.

Reimer, P.J., Austin, W.E.N., Bard, E., Bayliss, A., Blackwell, P.G., Bronk Ramsey, C., Butzin, M., Cheng, H., Edwards, R.L.,
Friedrich, M., Grootes, P.M., Guilderson, T.P., Hajdas, I., Heaton, T.J., Hogg, A.G., Hughen, K.A., Kromer, B., Manning,
S.W., Muscheler, R., Palmer, J.G., Pearson, C., van der Plicht, J., Reimer, R.W., Richards, D.A., Scott, E.M., Southon, J.R.,
Turney, C.S.M., Wacker, L., Adolphi, F., Büntgen, U., Capano, M., Fahrni, S.M., Fogtmann-Schulz, A., Friedrich, R., Köhler,
600   P., Kudsk, S., Miyake, F., Olsen, J., Reinig, F., Sakamoto, M., Sookdeo, A., Talamo, S.: The IntCal20 Northern Hemisphere
Radiocarbon Age Calibration Curve (0–55 cal kBP). Radiocarbon 62, 725-757, 2020.

Schweinsberg, A.D., Briner, J.P., Miller, G.H., Bennike, O., Thomas, E.K.: Local glaciation in West Greenland linked to North
Atlantic Ocean circulation during the Holocene. Geology 45, 195-198, 2017.

Schweinsberg, A.D., Briner, J.P., Miller, G.H., Lifton, N.A., Bennike, O., Graham, B.L.: Holocene mountain glacier history
605   in the Sukkertoppen Iskappe area, southwest Greenland. Quaternary Science Reviews 197, 142-161, 2018.

Seidenkrantz, M.S., Aagaard-Sørensen, S., Sulsbrück, H., Kuijpers, A., Jensen, K.G., Kunzendorf, H.: Hydrography and
climate of the last 4400 years in a SW Greenland fjord: implications for Labrador Sea palaeoceanography. The Holocene 17,
387-401, 2007.

Sinclair, G.: North Atlantic Climate and Cryosphere Variability Over the Past 20,000 Years, College of Earth, Ocean, and
610    Atmospheric Sciences. Oregon State University, 1-248, 2019.

Sparrenbom, C., Bennike, O., Björck, S., Lambeck, K.: Holocene relative sea-level changes in the Qaqortoq area, southern
Greenland. Boreas 35, 171-187, 2006.

Sparrenbom, C.J., Bennike, O., Fredh, D., Randsalu-Wendrup, L., Zwartz, D., Ljung, K., Björck, S., Lambeck, K.: Holocene
relative sea-level changes in the inner Bredefjord area, southern Greenland. Quaternary Science Reviews 69, 107-124, 2013.

615    Steenfelt, A., Kolb, J., Thrane, K.: Metallogeny of South Greenland: A review of geological evolution, mineral occurrences
and geochemical exploration data. Ore Geology Reviews 77, 194-245, 2016.

Stuiver, M., Reimer, P.J., and Reimer, R.W.: CALIB 8.2, http://calib.org, accessed 9/22/2022, 2022.

Weidick, A.: Ice Margin Features in the Julianehåb District, south Greenland. Reitzel, 1963.

Winsor, K., Carlson, A.E., Rood, D.H.: [10]Be dating of the Narsarsuaq moraine in southernmost Greenland: evidence for a late-
620    Holocene ice advance exceeding the Little Ice Age maximum. Quaternary Science Reviews 98, 135-143, 2014.

Wooller, M.J., Francis, D., Fogel, M.L., Miller, G.H., Walker, I.R., Wolfe, A.P.: Quantitative paleotemperature estimates from
d18O of chironomid head capsules preserved in arctic lake sediments. Journal of Paleolimnology 31, 267-274, 2004.